

Research laser system for resonance ablation of materials

A.N. Soldatov,^{1,2,3} A.V. Vasilieva,^{1,2,3} A.P. Ermolaev,¹ Yu.P. Polunin,¹
I.V. Sidorov,^{1,3} and A.G. Filonov^{1,3}

¹ Tomsk State University

² West-Siberian Branch of Russian State University for Innovation Technologies and Business, Tomsk

³ V.D. Kuznetsov Siberian Physical-Technical Institute at Tomsk State University, Tomsk

Received December 1, 2005

A system for investigations of the resonance laser ablation effect in polymers and biological tissues was designed, constructed, tested, and evaluated. The laser facility is based on a Sr-vapor laser operating at $\lambda = 6.456, 3.0665, 3.0111, 2.92, 1.0917, \text{ and } 1.0330 \mu\text{m}$. The system is capable of measuring laser output parameters varied in a wide range: average power between 1 and 10 W, pulse repetition rate between 1 and 20 kHz, pulse energy between 0.1 and 1 mJ, and energy density between 1 and 20 J/cm². Experimental data on the resonance laser ablation of polyamide-6 (caprolon) and muscular tissue (bovine muscle) are presented.

Introduction

Laser–matter interaction is one of the most important lines of investigations in modern optics and laser physics. This has considerably extended our views of fundamental photophysical processes at work in a material exposed to laser radiation of varying pulse duration and wavelength. What is more, the progress made in this research area has enabled physical principles underlying solutions to a large number of practical problems pertaining to lasers and their technological applications to be developed.

Today considerable study is being given to laser ablation, a process relevant to these fields of inquiry. The mechanisms behind this process are largely determined by laser output parameters. Several types of ablation are recognized (infrared, ultraviolet, resonance, and nonresonance) depending on the laser wavelength used and relation to the sample of interest. In addition, the ablation phenomenon is characterized by laser pulse duration. Here, exposure to femto-, nano-, or microsecond pulses is dealt with.

Of special interest is infrared resonance ablation, using nanosecond laser pulses. Analysis of the data available in the literature shows that the fundamental physical mechanisms responsible for the ablation process are not entirely known. However, there is evidence to suggest that infrared resonance ablation has a number of significant advantages over other kinds of laser–matter interactions. For instance, on exposure to ultraviolet radiation biological tissues experience side mutagenic effects that are not observed under infrared tissue irradiation.

We have developed a laser system to carry out investigations of the resonance ablation effect in biological tissues and polyamides in the mid-infrared region of the spectrum. The laser facility is based on a self-terminating atomic Sr-vapor laser.

1. Experimental data on laser ablation of bone tissues

Comparative experimental studies¹ on Ho:YAG, HF-, and CO₂-laser cutting of bone tissues revealed a laser-wavelength dependence of ablation results and enabled the term “resonance ablation” to be introduced. The mid-infrared laser spectrum proved to be best suited for cutting bone tissues. Further experiments on the laser wavelength tuning in the 2.9–9.2 μm range showed that the laser wavelength at 6.45 μm was particularly suitable for high-quality cutting of bone tissues, with the greatest cut depth (2.31 mm) produced without any charring of the tissue adjacent to the lesion. In our experiments, the laser-induced thermal damage zone was minimal (10–20 μm) for a cylindrical hole diameter of 200 μm .

It was found experimentally¹ that the hole depth was a function of the infrared absorption spectra in the 2.9–3.2 and 5.8–8.0 μm laser wavelength ranges for collagens, water, and calcium hydroapatites present in bone tissue. However, that was not the case with the infrared absorption spectra in the 8.9–9.2 μm range. To account for this fact, further investigations are necessary.

It was assumed in Ref. 1 that the ablation mechanism occurring below the plasma threshold in the case at hand was accomplished by explosive vaporization of water in closed space. In Refs. 2 and 3 it was pointed out that laser ablation of biological tissues took place at $\lambda = 3$ and 1 μm , which was attributed to strong absorption of laser radiation by the tissue water. This conclusion can be illustrated by considering the infrared absorption spectra of cornea, nerve tissue, and derma as examples.² A characteristic feature of these absorption spectra is that the OH-band mode lies near 3300 cm⁻¹ (3 μm). In addition, two more modes were detected: amide I,

the vibration mode of protein at 1665 cm^{-1} ($6\text{ }\mu\text{m}$) and amide II, the vibration mode of protein at 1550 cm^{-1} ($6.45\text{ }\mu\text{m}$). Notably, the ablation rate at $\lambda = 6.45\text{ }\mu\text{m}$ was higher and the collateral thermal damage was less severe than those found at $\lambda = 1$ and $3\text{ }\mu\text{m}$.

In the experiments under consideration, the light source was a free-electron laser (FEL) generating $4\text{ }\mu\text{s}$ macropulses consisting of 1–2 ps micropulse trains.^{1–3} The laser pulse repetition rate (PRR) was 30 Hz, and the pulse energy was 22.5 mJ, with the energy density deposited on the surface of the sample being 72 J/cm^2 (focal diameter was $200\text{ }\mu\text{m}$). The disadvantages of the laser are a sophisticated design, high cost, and large size, which prohibits its universal use in technological and medical investigations.

In order to gain insight into the resonance mid-infrared laser ablation effect, it is essential to have a laser source delivering a fairly high power at $\lambda = 1.3$, and $6.45\text{ }\mu\text{m}$. In this case, use can be made of a self-terminating low beam-divergence atomic Sr-vapor laser capable of producing a high single-pulse energy density. The PRR in this laser may be varied between 1 and several tens of kilohertz and the average output power may be 10 W and up.

2. Sr-vapor laser

We have used a self-terminating Sr-vapor laser (SrVL) in the ablation experiments under study. Laser action in the SrII (ionic) transitions at $\lambda = 3.01$ and $1.09\text{ }\mu\text{m}$, in the SrI (atomic) transitions at $\lambda = 6.45\text{ }\mu\text{m}$, and in those corresponding to $\lambda = 3.01$ and $3.06\text{ }\mu\text{m}$ was reported in Refs. 4 and 5. Lasing in the $4^3D - 5^3P^0$ triplet-triplet transitions at $\lambda = 2.60$, 2.69 , and $2.92\text{ }\mu\text{m}$ was discussed in Ref. 6. The highest average power produced in the SrVLs was 1 W.^{4–6} Experiments aimed at improving the SrVL output parameters were described in Refs. 7–10, where the maximum average power was 2–3 W and improvements in the specific and total energy characteristics of the lasers were shown to be feasible.

Thus the self-terminating SrVL action was observed at the following wavelengths⁶:

$$\lambda = 6.456\text{ }\mu\text{m} (5s5p^1P_1^0 - 5s4d^1D_2);$$

$$\lambda = 3.066\text{ }\mu\text{m} (5s4d^3D_1 - 5s5p^3P_2^o);$$

$$\lambda = 3.011\text{ }\mu\text{m} (5s4d^3D_2 - 5s5p^3P_2^o);$$

$$\lambda = 2.92\text{ }\mu\text{m} (5s4d^3D_3 - 5s5p^3P_2^o);$$

$$\lambda = 2.69\text{ }\mu\text{m} (5s4d^3D_2 - 5s5p^3P_1^o);$$

$$\lambda = 2.6\text{ }\mu\text{m} (5s4d^3D_1 - 5s5p^3P_0^o);$$

$$\lambda = 1.033\text{ }\mu\text{m} (4p^65p^2P_{3/2}^o - 4p^64d^2D_{3/2});$$

$$\lambda = 1.0917\text{ }\mu\text{m} (4p^65p^2P_{1/2}^o - 4p^64d^2D_{3/2}).$$

Record energy characteristics (total output power of 13.5 W, lasing power of 4.5 W near $3\text{ }\mu\text{m}$,

and lasing power of 1.9 W at two wavelengths near $1\text{ }\mu\text{m}$) were obtained in an active volume of 450 cm^3 (Ref. 11). The maximum total energy per laser pulse was 1.26 mJ for a PRR of 8.6 kHz. The feasibility of developing a high-power high-efficiency SrVL to generate simultaneous multiple-wavelength radiation in a wide PRR range was also shown.¹¹

3. Experimental setup

The laser system under consideration is designed for basic and applied research in the field of laser physics, biology, and materials science and engineering based on the mid-infrared laser ablation effect. The experimental setup consists of two parts: a test bench with two SrVL sources for low-PRR and high-PRR laser channels and a test bench for recording the laser radiation effect on the materials under study. The general view of the laser system is shown in Fig. 1.



Fig. 1. External view of the research SrVL system for resonance ablation of biological tissues and polymers.

Since we have been interested to perform experiments at varying laser output parameters, high- (10–20 kHz) and low-PRR (1–2 kHz) laser channels were used. Each channel includes an active SrVL element, a power supply, an unstable resonator, and a scanning unit. Two gas discharge tubes of respective bore diameters of 3 (GDT1) and 2.7 cm (GDT2) and of length 100 and 108 cm serve as active elements.

The optical layout of the system is demonstrated in Fig. 2 to illustrate the operation of the two laser channels. A low-divergence beam is formed by an unstable resonator 1. The average output power is measured by a power meter 4. The laser intensity distribution is determined by means of a limiting

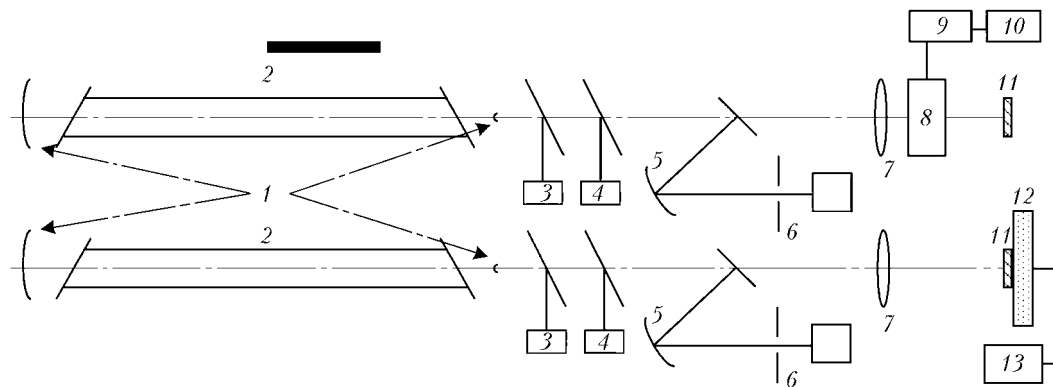


Fig. 2. Optical layout of the SrVL facility: unstable resonator mirrors (1), SrVL active element (2), photodetector (3), power meter (4), mirror (5), diaphragm (6), lens (7), scanner (8), scanner control unit (9), PC (10), target (11), translation stage (12), and translation stage control unit (13).

diaphragm 6. The divergence across the beam is estimated from the spot diameter in the focal plane of a mirror with a focal length of 5 m. The beam is focused on a target 11 fixed on a motorized translation stage 12, using a lens 7 with a focal length of 0.1 m. The mode of operation of the translation stage is set by a control unit 13.

The high-PRR channel includes the same components as the low PRR channel does. The only difference is that a scanner 8 connected to a computer 10 is placed behind the lens 7 in the former channel. The scanner sets the path of the laser beam incident on the target 11 placed at the focus of the lens 7. For simplification of the schematic representation of the system, diffraction gratings designed for spectral separation of lasing lines generated by the two laser light sources are omitted. However, wavelength selection can be accomplished not only by means of the optics, but also by varying the mode of the laser operation. Under normal operating conditions, 90% of the SrVL radiation is due to the wavelength at 6.45 μm , but there are regimes of laser operation where the fractions of radiation at $\lambda = 3$ and 1 μm are dramatically increased.

A unique feature of the SrVL used in the system is the multiple-wavelength (8 operating wavelengths) laser action. This enables the ablation process to be investigated during interactions of laser radiation with different types of biological tissues and with polyamides containing amide groups. The combination of the wavelengths generated by the lasers and the possibility of controlling the percentage of the average power generated at individual laser wavelengths makes it possible to reveal the wavelength effect on the ablation process.

Basic technical data for the laser system under consideration are summarized below.

Laser wavelength, μm	1.03; 1.09; 2.60; 2.69; 2.92; 3.01; 3.06; 6.45
Laser beam divergence, mrad	0.5

Laser pulse duration, ns	30–50
Pulse repetition rate, kHz:	
high PRR channel	10–20
low PRR channel	1–2
Total pulse energy for all laser wavelengths, mJ	
(low-PRR channel)	1
Average lasing power, W	
(high-PRR channel)	10
Energy density, J/cm^2	1–20
Power consumption, kW	5
Cooling medium	air

The laser system under consideration also incorporates measurement devices to control laser output parameters and an 8 Mpixel photcamera with an added objective to record ablation results through the control unit.

4. SrVL ablation

4.1. Low laser-energy ablation results

Early experiments on SrVL-ablation of biological tissue were reported in Ref. 11. The average laser power, PRR range, pulse energy, and focal diameter were 2.4 W, 5–20 kHz, < 185 μJ , and 130 μm , respectively. The laser was of small size. The low pulse energy was found to limit the possibility for variation of laser output parameters.

The laser was placed on an optical table (Newport Inc., Irvine, CA). Laser light was directed to an off-axis parabolic mirror ($f = 25.4$ mm) that focused the beam on a translation stage. The laser energy was measured by a 365 Scientech power meter (Scientech, Boulder, CO). The focal diameter was measured, using a knife-edge technique. A water-filled cuvette was mounted on the translation stage moving in a straight line. Images of the ablation process were recorded onto a videotape by means of a standard black-and-white CCD camera with a frame rate of 30 Hz. The images were then digitized with the use of an ATI Rage-Pro Mobility videocard for further processing and analysis.

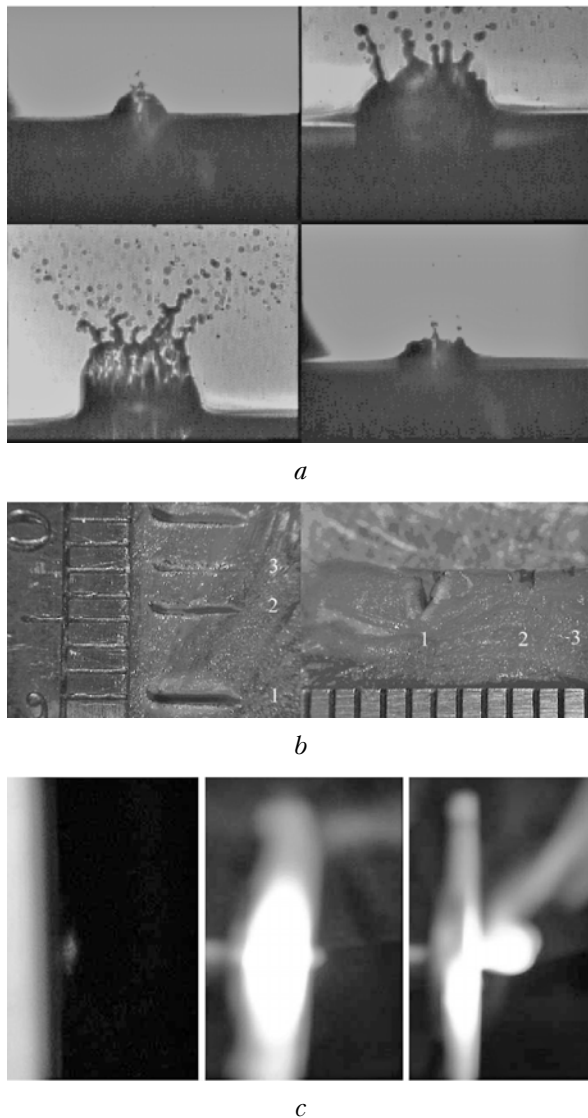


Fig. 3. Images of SrVL ablation of water: PRR = 13 kHz, average power $P_{av} = 2$ W (a); enlarged images of bovine muscle exposed to SrVL radiation (b): lesion 1 (PRR = 16 kHz, $P_{av} = 2.4$ W, the spot size is 130 μm in diameter, the scan rate is 17 mm/s, 30 passes); lesion 2 (PRR = 5 kHz, $P_{av} = 0.9$ W, the spot size is 130 μm , the scan rate is 17 mm/s, 30 passes); lesion 3 (PRR = 5 kHz, $P_{av} = 0.9$ W, the spot size is 130 μm , the scan rate is 17 mm/s, 10 passes), and the time history of the ablation plume for caprolon (c).

The time history of ablation of water is illustrated in Fig. 3a. Four frames show the onset of the ablation event, expansion of the vapor cavity, ejection of water, and collapse of the vapor cavity.

Bovine muscle was examined under the microscope (Fig. 3b). Small strips of the tissue were placed at the focus of the laser beam on the translation stage. The stage was moved back and forth throughout the ablation process to produce 4-mm long linear lesions. The laser parameters and the rate of motion of the stage were varied for comparison. The lesions were viewed through a microscope and imaged.

The tissue was ablated during the course of several pulses to produce a thermal effect in the surrounding tissue. This is assumed to be related with the high laser PRR. It is seen from Fig. 3b that higher ablation yield is obtained as PRR is increased. However, more severe collateral thermal injury to the tissue is observed in this case.

The results obtained testify that the SrVL can be used for resonance ablation, even though the SrVL mode of operation differs essentially from that of a FEL. To this end, the SrVL pulse energy and beam quality must be improved to minimize the side effects and increase the ablation rate.

4.2. Laser ablation at increased SrVL energy parameters

4.2.1. Experimental tests

The research SrVL system was tested and evaluated. In the experiments, pumping conditions, composition of the active medium of the laser sources used in the two channels, and ways of forcing the lasers into the operating mode were varied. Selected results of experiments using low- and high-PRR laser channels are listed in Table 1.

The SrVL output energy characteristics in different spectral lines depend on a number of parameters: buffer gas species and pressure, Sr-vapor pressure, electric field strength, etc. The average lasing power at $\lambda = 6.45$ μm was found to increase in a gradual manner with increase in the buffer gas pressure, the electric field strength being kept unchanged.

Table 1. Experimental results for low- and high-PRR laser channels

GDT	Total lasing power, W	PRR, kHz	Pulse energy, mJ	Lasing power, W, at individual laser wavelengths, μm		
				6.45	~ 3	~ 1
$V = 706$ cm^3 $d = 3$ cm	6.5	—	—	4.35	1.5	0.65
	8	14.5	0.6	7	0.2	0.1
	10.5	15	0.7	—	—	—
$V = 618$ cm^3 $d = 2.7$ cm	2.6	2.2	1.2	—	—	—
	4.2	3	1.4	—	—	—
	5	—	—	3.37	1.4	0.23

The lasing power in the other lines remained practically constant. The lasing power at $\lambda = 6.45$ and near $3 \mu\text{m}$ was higher in the case of helium used as buffer gas than with neon, the excitation conditions being the same.

The percentage of the average power at different laser wavelengths was examined as a function of the GDT heat time in an active volume of 618 cm^3 . As illustrated in Fig. 4, the fraction of the laser radiation emitted at $\lambda = 6.45 \mu\text{m}$ increases linearly with the GDT temperature. It is evident from the curves that the power at $\lambda = 6.45 \mu\text{m}$ continues to increase with further increase in the GDT temperature.

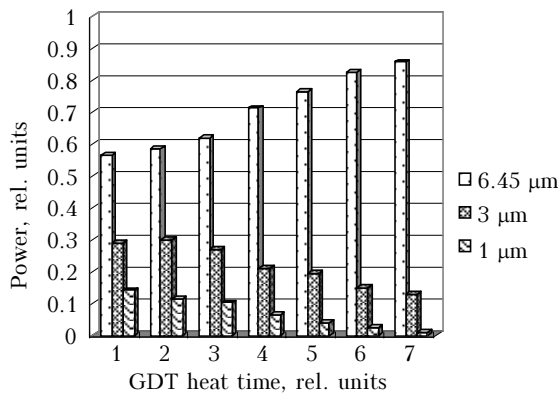


Fig. 4. Lasing power at $\lambda = 6.45$, ~ 3 , and $\sim 1 \mu\text{m}$ as a function of GDT heat time in the SrVL laser with the total power normalized by unity.

4.2.2. Laser ablation of polyamides

The SrVL-based facility under consideration was used in the preliminary stage of experiments on the laser radiation effect on polyamides. The series of studies enabled resonance ablation of polyamide-6 (known as caprolon) to be obtained. The experimental data are summarized in Table 2. The cut width was varied between 120 and $150 \mu\text{m}$ and the melting zone was several tens of nanometers. As pointed out in many papers, a distinguishing feature of the ablation process is the formation of an ablation plume that was observed directly in the course of our experiments as well (Fig. 3c).

Summary

Resonance laser ablation is a peculiar type of ablation of materials characterized by a minimum collateral damage and a maximum ablation rate, as contrasted to nonresonance ablation.

We have performed resonance laser ablation of water and bovine muscle and of polyamide-6, using low and high laser energy parameters, respectively. While in the former case ablation was observed, a profound thermal effect was produced largely due to the insufficient lasing pulse energy.

Thus, it was found experimentally that efficient resonance SrVL ablation of materials can be accomplished with the proviso that the laser source used is capable of

(1) emitting radiation at a resonance wavelength,

(2) producing an energy density above the ablation threshold for the material under study,

(3) generating high-quality high-uniformity low-divergence beams of light.

The self-terminating atomic SrV laser meets these requirements and can be used to advantage for resonance ablation of biological tissues and polyamides.

A special feature of the laser system developed on the basis of the experimental results is the lasing spectrum that includes 8 wavelengths in the range from 1 to $6.45 \mu\text{m}$. These are of scientific interest, because they fall at the maximum absorption bands of biological tissues.

The energy parameters of the SrVL sources used in the system were dramatically increased. The average output power can be varied between 1 and 10 W. The PRR varied in a wide range (1–20 kHz) for pulse energies of 0.1–1 mJ makes it possible to investigate in detail the effect of high PRRs on the efficiency of the laser ablation process. In this case, an energy density of $20 \text{ J}/\text{cm}^2$ is generated owing to high output beam quality.

The results obtained in the preliminary stage of the experiments show that the system under consideration holds much promise for resonance laser ablation of materials. This is exemplified by ablation of bovine muscle tissue and polyamide-6 (caprolon).

Table 2. Experimental data on ablation of polyamide-6

PRR, kHz	Average power, W	Pulse energy, mJ	Focal diameter, μm	Energy density, J/cm^2	Cut depth, μm	Cut width, μm	Ablation rate, $\mu\text{m}/\text{pulse}$
15	5.7	0.38		4.8	22	150	2.2
2	1	0.5		6.4	50	130	5
15	10	0.6	100	7.6	55	130	5.5
1.5	2	1.3		16.6	104	120	10.4
8.6	13.5	1.56		19.8	115	120	11.5

Acknowledgments

We gratefully acknowledge support of this work by the RF Science and Innovation Agency (Grant No. 09.255.02/065).

References

1. G.M. Peavy, I. Reinisch, J.T. Payne, and I. Venigopalan, *Lasers in Surgery and Medicine* **25**, 421–434 (1999).
2. G.S. Edwards, R.H. Austin, F.E. Carroll, et al., *Rev. Sci. Instrum.* **74**, No. 7, 3207–3245 (2003).
3. B. Majaron, P. Plestenjak, and M. Lukac, *Appl. Phys.* **B69**, No. 1, 71–80 (1999).
4. A.V. Platonov, A.N. Soldatov, and A.G. Filonov, *Sov. J. Quant. Electron.* **8**, No. 1, 120–122 (1978).
5. P.A. Bokhan and V.D. Burlakov, *Sov. J. Quant. Electron.* **9**, No. 3, 374–376 (1979).
6. B.-L. Pan, G. Chen, J.-W. Zhong, and Z.-X. Yao, *Appl. Phys. B*, No. 76, 371–374 (2003).
7. A.N. Soldatov, I.I. Plusnin, and A.G. Filonov, in: *Proc. of the 5th Russian-Chinese Symp. on Laser Phys. and Laser Tech.* (Tomsk, 2001), p. 303.
8. T.M. Gorbunova, A.N. Soldatov, and A.G. Filonov, *Atmos. Oceanic Opt.* **17**, Nos. 2–3, 231–234 (2004).
9. A.N. Soldatov, A.G. Filonov, A.S. Shumeiko, et al., *Proc. SPIE* **5483**, 252–261 (2003).
10. A.N. Soldatov, Yu.P. Polunin, A.S. Shumeiko, and I.V. Sidorov, in: *Proc of the 7th Int. Symp. on Laser Phys. Laser Tech.* (Tomsk, 2004), pp. 202–207.
11. M.A. Mackanos, B. Ivanov, A.N. Soldatov, et al., *Proc. SPIE* **5483**, 252–261 (2003).